

A Multi-State Diagnosis and Prognosis Framework with Feature Learning for Tool Condition Monitoring

Chong Zhang, *Student Member, IEEE*, Geok Soon Hong, Jun-Hong Zhou, Kay Chen Tan, *Fellow, IEEE*, Haizhou Li, *Fellow, IEEE*, Huan Xu, Jihoon Hong, *Member, IEEE*, and Hian-Leng Chan

Abstract—In this paper, a multi-state diagnosis and prognosis (MDP) framework is proposed for tool condition monitoring via a deep belief network based multi-state approach (DBNMS). For fault diagnosis, a cost-sensitive deep belief network (namely ECS-DBN) is applied to deal with the imbalanced data problem for tool state estimation. An appropriate prognostic degradation model is then applied for tool wear estimation based on the different tool states. The proposed framework has the advantage of automatic feature representation learning and shows better performance in accuracy and robustness. The effectiveness of the proposed DBNMS is validated using a real-world dataset obtained from the gun drilling process. This dataset contains a large amount of measured signals involving different tool geometries under various operating conditions. The DBNMS is examined for both the tool state estimation and tool wear estimation tasks. In the experimental studies, the prediction results are evaluated and compared with popular machine learning approaches, which show the superior performance of the proposed DBNMS approach.

Index Terms—Tool Condition Monitoring (TCM), Diagnostics, Prognostics, Deep Belief Network, Multi-state.

I. INTRODUCTION

Tool condition monitoring (TCM) has become indispensable to smart manufacturing, automated machining, and other industrial processes nowadays. It not only reduces unnecessary machine downtime and maintenance costs, but also improves the quality and precision of the product. The TCM framework provides diagnostics and prognostics to estimate tool states (e.g. fresh, progressive wear, accelerated wear, worn, etc.) and predict tool wear.

The idea of TCM is to monitor the health condition of the tool continuously using data analytics. Signals such as force, torque, vibration and acoustic emission can be collected and monitored using various sensors mounted on the machinery

systems. The data-driven approaches have become a mainstream solution to TCM. They make use of computational intelligence, machine learning or deep learning models that learn from run-to-failure historical data from the system. Such approach can learn the knowledge from data without domain knowledge. Since a perfectly defined physical model of tool wear is not available, data-driven approaches are appealing in practice.

Among the data-driven approaches to TCM, conventional machine learning methods such as neural networks (NNs) [1], Gaussian process regression [2], make use techniques that are common in pattern classification, such as feature extraction and feature selection. For instance, the selected features are further used as input to NNs for classification or regression tasks. While these conventional methods work in many tool condition monitoring applications, they suffer from two shortcomings. Firstly, the features are manually extracted highly relying on prior domain knowledge. Moreover, the hand-crafted features extracted from one application scenario may not be generalized to other scenarios. Secondly, due to their shallow architectures, conventional NNs have a limited ability of learning complex non-linear prediction in diagnostics and prognostics. We consider that deep belief networks (DBNs) [3], [4] have the potential to overcome the aforementioned shortcomings. DBNs with unsupervised generative feature learning could be able to mine the useful information from raw data and approximate complex non-linear mappings between raw data and the tasks.

There are two main tasks, namely diagnosis and prognosis, dichotomized the prediction process in TCM system. The previous studies have mostly focused on either diagnosis or prognosis in TCM [5], [6]. Diagnosis is to estimate what the current health state is. Prognosis is to predict what will happen next. Prognostics is the study as to show how the tool condition degrades and to estimate the remaining useful life (RUL) of the tool. With effective and reliable estimation of RUL, TCM can reduce overall downtime of the manufacturing processes. Although prognostics plays an important role in TCM, it still a lukewarm research area with few reported studies. In a TCM system, the tool wear estimation forms the basis of tool RUL estimation. In this paper, we would like to focus on tool state estimation as the main diagnostics task and tool wear estimation as the main prognostics task.

The performance of prognosis can be improved based on more accurate current health state estimation. Because the

C. Zhang and H. Li are with the Department of Electrical and Computer Engineering, G. S. Hong and H. Xu are with the Department of Mechanical Engineering, National University of Singapore, 4 Engineering Drive 3, 117583, Singapore. (e-mails: zhangchong@u.nus.edu; haizhou.li@nus.edu.sg; mpehgs@nus.edu.sg; xuhuan@u.nus.edu)

K. C. Tan is with the Department of Computer Science, City University of Hong Kong, 83 Tat Chee Avenue, Kowloon, Hong Kong. (e-mail: kaytan@cityu.edu.hk)

J. Zhou, J. Hong and H. L. Chan are with the Singapore Institute of Manufacturing Technology (SIMTech), Agency of Science Technology and Research (A*STAR), 638075 Singapore. (e-mails: jzhou@simtech.a-star.edu.sg; hongjh@simtech.a-star.edu.sg; hlchan@simtech.a-star.edu.sg)

This paper has been submitted to IEEE Transactions on Cybernetics in Dec 2017.

degradation trends of the system/components may be different based on different current health states, the results of diagnostics and prognostics are tightly related with the overall performance of the TCM system. Since the distribution of data in different health states are naturally multifarious, any single model is quite hard to handle them. We consider that multi-state diagnosis and prognosis framework distinguishes health states in finer details, that allows us to apply different models according to the diagnostic data attributes. We have a good reason to believe that such multi-modal approach offers better performance. Therefore, this paper proposes a multi-state diagnosis and prognosis framework (MDP) based on tool state estimation by fault diagnosis to provide more reliable and accurate prognostic prediction in tool condition monitoring, namely tool state classification and tool wear estimation.

This paper is organized as follows. Section II reviews current related literature. Section III introduces the proposed multi-state diagnosis and prognosis framework and a deep belief network based multi-state approach. Section IV describes the details of the real-world gun drilling dataset in the aspects of experimental setup, data acquisition and data preprocessing. Section V presents the evaluation metrics of diagnostics and prognostics, respectively. Section VI presents and analyzes the experimental results of tool state estimation and tool wear estimation as well as the comparison with other methods on the real-world gun drilling dataset. Section VII concludes this paper and highlights some potential future research directions.

II. LITERATURE REVIEWS

Generally, TCM approaches are categorized into physical-based approaches, data-driven approaches and hybrid approaches. Physical-based approaches are highly depending on expert domain knowledge. However, in many complex systems, it is hard to establish well-defined mathematical models. Moreover, physical-based approaches [7] are only suitable for certain operating conditions and lack of generalization capability to suit the model for different conditions. Data-driven approaches are based on historical data and require less domain knowledge. Data-driven approaches [8], [9] usually use artificial/computational intelligence techniques such as neural network [1], [10], [11], Gaussian process regression [2], support vector machine [12], [13], fuzzy inference techniques [14], [15], etc. Hybrid approaches [16], [17] attempt to combine physical-based approach and data-driven approach together.

In the early studies, many data-driven approaches [18]–[25] made binary tool state (i.e., healthy and faulty) estimation. Li et al. [26] proposed a TCM framework utilized neuro-fuzzy techniques to estimate the feed cutting force based on the measured feed motor current. Neural networks (NNs) are also popular used on TCM frameworks to generate non-linear mapping between inputs and outputs. [27] applied NN for fault diagnosis. Zhu et al. [28] proposed an online TCM framework based on force waveform feature extraction.

Hidden Markov Model (HMM) based approaches [23], [29]–[33] are widely used in TCM. PS-HMCO [23] is a temporal probabilistic physically segmented approach based on

HMM for prognostics. This approach is effective by using multiple physically segmented HMM in parallel with each HMM focusing on a different tool wear regiment. VDHMM [31] is an adaptive-Variable Duration Hidden Markov Model to adapt with different cutting conditions for prognostics. Recently, Zhu et al. [32] proposed a hidden semi-Markov model (HSMM) with dependent durations for online tool wear monitoring with online tool wear estimation and RUL estimation. However, feature extraction and selection are needed for HSMM.

Based on the similar rationale, key feature based approaches [28], [34], [35], probabilistic and neural networks approaches [36], [37], linear discriminant analysis [38], switching Kalman filter [39], [40], and genetic programming [41] are applied to fault diagnosis and RUL estimation.

However, all of the aforementioned approaches require well-defined hand-crafted features and their performances are highly relying on the quality of the manually extracted features. Some approaches such as [19], [42] cannot accomplish multiclass tool state classifications to reach the high precision and quality requirements in manufacturing processes. In addition, the aforementioned approaches are only suitable for fixed operating conditions and they did not address flexibility and generalization problems.

III. MULTI-STATE DIAGNOSIS AND PROGNOSIS FRAMEWORK FOR TOOL CONDITION MONITORING

This paper proposes a novel multi-state diagnosis and prognosis framework (MDP). The schematic diagram of the MDP for TCM decision making is shown in Fig. 1.

There could be different ways to implement the MDP framework. We suggest a deep belief network based multi-state approach to the problem, that we call DBNMS. We formulate the DBNMS as a pipeline process. We first identify the tool states using evolutionary cost-sensitive deep belief network (ECS-DBN) which is suitable for imbalanced data classification [43]–[45], then based on different tool states choose appropriate DBN models for more accurate and robust tool wear estimation based on the tool states, finally we make reliable decisions based on the accurate estimates. DBNMS includes two main steps. In the first step, we carry out fault diagnosis where ECS-DBN is used to handle imbalanced data problem. In the second step, we carry out fault prognosis by using appropriate DBN models to learn feature representations automatically. In practice, the distribution of data samples obtained from different tool states may vary and skew, conventional classifiers often fail to classify minority classes due to imbalanced training data. In the DBNMS implementation, the raw data are taken to the system only with the standard time-windowing and normalization. Thus, DBNMS can be considered as an end-to-end deep learning solution to the TCM problem.

Fig. 2 compares different frameworks including physical-based framework, conventional data-driven based framework and deep learning based framework. Each round box in the figure denotes a data-driven process. Traditional physical-based framework requires strong domain knowledge to hand design physical models while data-driven based frameworks

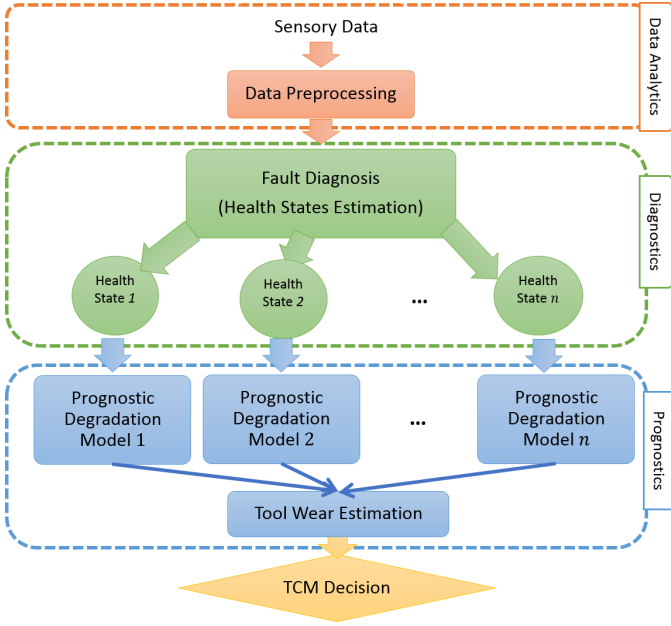


Fig. 1. Schematic diagram of multi-state diagnosis and prognosis framework (MDP) for tool condition monitoring.

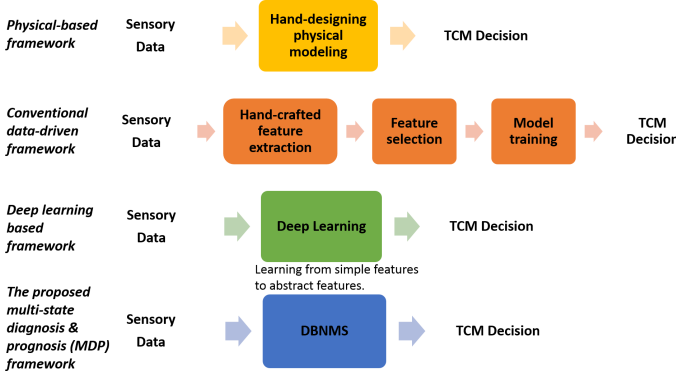


Fig. 2. Comparison of four different frameworks, i.e., physical-based, conventional data-driven based, deep learning based and MDP. Round boxes denote algorithm/computing modules.

only require historical data with less domain knowledge. For some complex systems/components, it is quite hard to formulate precise physical models. In contrast, it is more feasible to obtain data such as sensor signals, operational conditions, event data which are related to the health conditions of the systems/components. Therefore, data-driven framework is applicable for such kind of applications. From Fig. 2, it is obvious that deep learning based framework is an end-to-end framework with automatic feature learning comparing with conventional data-driven based framework. Conventional data-driven framework needs extensive human labor for hand-crafted features and has several tedious individual modules which need to be trained step-by-step. Deep learning based framework has automatic feature representation learning without hand-crafted features. All of its parameters are trained jointly. It is suitable for large-scale data.

In this section, MDP framework for diagnostics and prognostics in TCM is proposed and presented in details. The

proposed MDP framework incorporates with fault diagnosis and tool wear estimation tasks. Diagnosis is the task of estimating the health state of the system/component at the current time stamp given all historical data. Prognosis is the task of predicting the wear of the tool in future time stamp.

A. Fault Diagnosis: Tool State Estimation

Fault diagnosis is to estimate current health state of the tools based on current and historical data. It is essentially a classification problem. Many existing studies only assume binary tool states which are fresh and worn. However, such assumption does not allow for accurate and robust predictions. We consider that tool wear is a progressive process, thus, the state of tool wear is multiclass. We also note that the number of data sample obtained during faulty state of the tool is always far less than that of healthy state of the tool. The minority data are always more important because misclassifying them will cause fatal failure and highly costs. Thus there is a need to address imbalanced data problem. Unfortunately, the conventional algorithms such as neural network, DBN generally assume all misclassification costs are equal which is not suitable for such problem. We note that in many real-world applications, misclassification costs are usually unknown and hard to be decided. We suggest using ECS-DBN to address the imbalanced data problem in fault diagnosis. ECS-DBN proposed by Zhang et al. [43], [44] incorporating cost-sensitive function directly into its classification paradigm and utilizing adaptive differential evolution for misclassification costs optimization is shown good performance on handling imbalanced data problems on many popular benchmark datasets.

1) *Multiclass Classification of Tool States*: Each class in the multiclass classification corresponds to a tool state. We propose a multi-state description to provide more detailed representation of tool wear process. The health state of a tool is fresh and sharp in the initial wear stage, and the tool wear increases progressively with cutting time, then its flank wear rapidly reaches accelerated wear region, eventually it worn after the accelerated wear region. In contrast, the binary classification of tool states (i.e., fresh and worn tool states) may not be able to reflect this wearing process accurately. In addition, multiclass classification of the tool states can improve the final performance of the proposed framework by splitting tool states more precisely so as to avoid unnecessary tool replacement or workpiece damage.

In this paper, the number of classes or states are chosen based on domain knowledge in machinery. According to the size of flank wear, four classes are suggested as shown in Table I. When the average flank wear V_B is less than or equal to $100\mu m$, the tool is considered as fresh. The progressive wear region of the tool is between $100\mu m$ to $200\mu m$. The accelerated wear region of the tool is between $200\mu m$ to $300\mu m$. The tool is considered as worn when its flank wear is equal or more than $300\mu m$. The tool should be replaced immediately when it is worn to avoid workpiece damage and ensure the product quality.

2) *Evolutionary Cost-sensitive Deep Belief Network (ECS-DBN)* [43]: Assume the total number of classes is n , given

TABLE I
TOOL STATES CATEGORIZED BY FLANK WEAR.

| Class | Flank Wear (V_B) | Tool State |
|-------|-----------------------------------|------------------|
| 0 | $V_B \leq 100\mu m$ | Fresh |
| 1 | $100\mu m \leq V_B \leq 200\mu m$ | Progressive Wear |
| 2 | $200\mu m \leq V_B \leq 300\mu m$ | Accelerated Wear |
| 3 | $V_B \geq 300\mu m$ | Worn |

a sample data \mathbf{x} , $C_{i,j}$ denotes the cost of misclassifying x as class j when x actually belongs to class i . In addition, $C_{i,j} = 0$, when $i = j$, which indicates the cost for correct classification is 0. The meaning of the element $C_{i,j}$ is the misclassification costs of predicting class i when the true class is j .

Given the misclassification costs, a data sample should be classified into the class that has the minimum expected cost. Based on decision theory [46], the decision rule minimizing the expected cost $\mathcal{R}(i|\mathbf{x})$ of classifying an input vector \mathbf{x} into class i can be expressed as:

$$\mathcal{R}(i|\mathbf{x}) = \sum_{j=1}^n P(j|\mathbf{x})C_{i,j}, \quad (1)$$

where $P(j|\mathbf{x})$ is the posterior probability estimation of classifying a data sample \mathbf{x} into class j . According to the Bayes decision theory, an ideal classifier will give a decision by computing the expected risk of classifying an input to each class and predicts the label that reaches the minimum expected risk. In the traditional learning algorithms, generally all costs are assumed to be equal. In cost-sensitive learning, all costs are non-negative.

However, in real-world applications, the misclassification costs are essentially unknown and nonidentical among various classes. The previous studies [47] usually attempt to determine misclassification costs through try-and-error, that generally does not lead to optimal misclassification costs. Some studies [48] have designed some mechanisms to update misclassification costs based on the number of samples in different classes. However, this kind of methods may not suitable for some cases where some classes are important but rare, such as some rare fatal diseases. To avoid hand tuning of misclassification costs and achieve optimal solution, adaptive differential evolution algorithm [49] has been implemented in this paper. Adaptive differential evolution algorithm is a simple yet effective evolutionary algorithm which could obtain optimal solution by evolving and updating a population of individuals during several generations. It can adaptively self-updating control parameters without prior knowledge.

Mathematically, the probability that a sample data $\mathbf{x} \in S_{data}$ belongs to a class j , a value of a stochastic variable y , can be expressed as as a softmax function:

$$P(j|\mathbf{x}) = P(y = j|\mathbf{x}) = \frac{\exp(\mathbf{b}_j + \mathbf{W}_j \mathbf{x})}{\sum_i \exp(\mathbf{b}_i + \mathbf{W}_i \mathbf{x})}, \quad (2)$$

where \mathbf{b} and \mathbf{W} respectively are bias and weights within the network. Implement the misclassification costs C on the

obtained probability $P(y = j|C, W, b)$, then it can obtain the cost function:

$$P_\xi = \sum_{i=1}^n P(y = j|\mathbf{x}) \cdot C. \quad (3)$$

The hypothesis prediction of the sample ζ is the member of the minimum probability of misclassification among classes, can be obtained by using the following equation:

$$\zeta = \arg \max_j P_\xi(y = j|\mathbf{x}). \quad (4)$$

Note that the ECS-DBN only focuses on output layer. For the pre-training phase and fine-tuning phase, the method implemented in this paper is the original greedy layer-wised pre-training method proposed by Hinton [3].

The procedure of training ECS-DBN is presented as follows. Firstly, we randomly initialize a population of misclassification costs. Secondly, we use the training set to train a DBN. After applying misclassification costs on the outputs of the networks, we evaluate the training errors based on the performance of the corresponding cost-sensitive hypothesis prediction. Thirdly, according to the evaluation performance on training set, we select proper misclassification costs to generate the population of next generation. Fourthly, in the next generation, we use mutation and crossover operator to evolve a new population of misclassification costs. Adaptive DE algorithm [50], [51] will proceed to next generation and continue the mutation to selection until the maximum generation is reached. Eventually, we obtain the best misclassification costs and apply it on the output layer of DBN to form ECS-DBN. At run-time, we test the resulting cost-sensitive DBN with test dataset to report the performance.

In ECS-DBN, each chromosome represents misclassification costs for each class, and the final evolved best chromosome is chosen as the misclassification costs for ECS-DBN. The misclassification costs are used to encode into the chromosome with numerical type and value range of $[0, 1]$. G-mean of training set is chosen as the objective to be maximized for ECS-DBN on training dataset. A maximum number of generation is set as the termination condition of the algorithm. The algorithm is terminated to converge upon the optimal solution. At the end of the optimization process, the best individual is used as misclassification costs to form an ECS-DBN. Then test the performance of the generated ECS-DBN on test dataset.

B. Prognostics: Tool Wear Estimation

There are many existing algorithms which can be used as the degradation model such as linear or non-linear regression methods, neural networks [40], [52], support vector machine [53], [54], switching Kalman filter [39] and so on. However, those conventional methods are highly relying on hand-crafted features and cannot provide an effective feature representation learning. We consider that a DBN with the unsupervised feature learning techniques allows us to automatically learn features that could be more suitable to establish a framework with better feature representation learning. Here

a DBN is used as a regressor to estimate the tool wear. The inputs of DBN are preprocessed data calculated by presence and past signals. Its outputs are the estimated tool wear value in the next time step.

Deep belief network (DBN) proposed by Hinton et al. [3] contains multiple hidden layers and each hidden layer constructs non-linear transformation from the previous layer with minimum reconstruction errors. Typically, DBNs are trained with two main procedures, i.e., unsupervised pre-training and supervised fine-tuning. The fundamental building block of DBN is Restricted Boltzmann Machine (RBM) which consists of one visible layer and one hidden layer. To construct DBN, hidden layer of anterior RBM is regarded as the visible layer of its posterior RBM. DBN is stacked with several RBMs and its architecture allows to abstract higher level features through layer conformation.

In RBM, the joint probability distribution of (\mathbf{v}, \mathbf{h}) of the visible and hidden units has an energy given by [55]:

$$E(\mathbf{v}, \mathbf{h}) = - \sum_{i \in \text{visible}} a_i v_i - \sum_{j \in \text{hidden}} b_j h_j - \sum_{i,j} v_i h_j w_{ij}, \quad (5)$$

where v_i, h_j denote the states of visible unit i and hidden unit j . a_i, b_j are their biases and w_{ij} represent the weight between them. Probabilities have been allocated among connections pairs visible and hidden units via function:

$$p(\mathbf{v}, \mathbf{h}) = \frac{e^{-E(\mathbf{v}, \mathbf{h})}}{\sum_{\mathbf{v}, \mathbf{h}} e^{-E(\mathbf{v}, \mathbf{h})}}. \quad (6)$$

The possibility of the state of hidden vector \mathbf{h} given by a randomly input visible vector \mathbf{v} is as

$$p(h_j = 1 | \mathbf{v}) = \text{sigmoid}(b_j + \sum_i v_i w_{ij}), \quad (7)$$

where sigmoid function denotes $f(x) = \frac{1}{1+e^{-x}}$. The possibility of the state of visible vector \mathbf{v} given by the previous obtained hidden vector \mathbf{h} is followed by

$$p(v_i = 1 | \mathbf{h}) = \text{sigmoid}(a_i + \sum_j h_j w_{ij}). \quad (8)$$

The widely used contrastive divergence [56] algorithm is used to update the weights and biases.

IV. DATASET

In this paper, a real-world gun drilling dataset is used as a case study under the proposed framework. The dataset was acquired with a UNISIG USK25-2000 gun drilling machine in the Advanced Manufacturing Lab at the National University of Singapore in collaboration with SIMTech-NUS joint lab.

A. Experimental Setup

In the experiments, an Inconel 718 workpiece with the size of $1000\text{mm} \times 100\text{mm} \times 100\text{mm}$ is machined using gun drills. Inconel 718 is widely used in Jet engines. The tool diameter of gun drills is 8mm . The details of tool geometry can be found in Table II. The experimental setup and layout are shown in Fig. 3 and Fig. 4, respectively. Four vibration sensors (Kistler Type 8762A50) are mounted on the workpiece in order

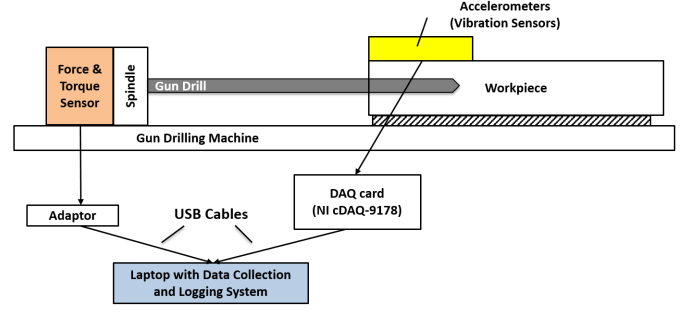


Fig. 3. Illustration of the experimental setup of gun drilling experiments with force, torque and vibration sensors. The force and torque sensor is placed on end of the tool. The four accelerometers (vibration sensors) are placed on top of the workpiece, then connected to a DAQ card. Finally, a laptop is used for data collection and data logging.

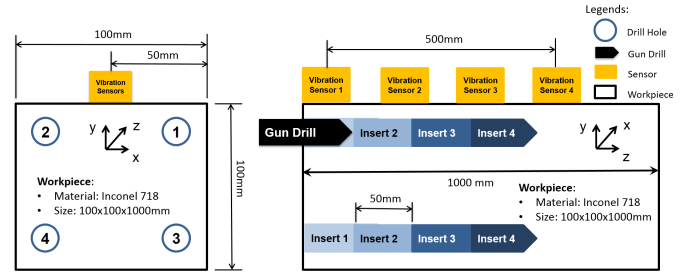


Fig. 4. Illustration of the front (on the left) and side (on the right) views of the workpiece and sensor layouts in gun drilling experiment. Note that the z axis is the same with gun drilling direction.

to measure the vibration signals in three directions (i.e., x , y and z) during the gun drilling process. The details about sensor types and measurements are summarized in Table III. The sensor signals are acquired via a NI cDAQ-9178 data acquisition device and with a laptop Dell Latitude E5450 that has an Intel Core i7-5600U 3.20GHz CPU.

During data acquisition, 14 channels of raw signals belonging to three types are logged. The measured signals include force signal, torque signal, and 12 vibration signals (i.e., acquired by 4 accelerometers in x, y, z directions) as shown in Fig. 5 and Fig. 6. The tool wears have been measured using Keyence VHX-5000 digital microscope. In this paper, the maximum flank wear has been used as the health indicator of the tool. In this dataset, it is found 3 out of 20 tools are broken, 6 out of 20 tools chip at final state and 11 out of 20 tools wear after gun drilling operations.

The machining operation is carried out with the detailed hole index, drill depth, tool geometry, tool diameter, feed rates, spindle speeds, machining times and tool final states are shown in Table II. The drilling depth of each insert is 50 mm in z -axis direction. The tool wear is captured and measured by Keyence digital microscope. The tool wear is measured after each drill during gun drilling operations. Since the aim of this benchmark dataset attempts to cover more diverse conditions, the tool geometry of different tools are varied.

B. Data acquisition experiments

To collect the data, we conduct experiments that are schematically shown in Fig. 7. The details of the gun drilling

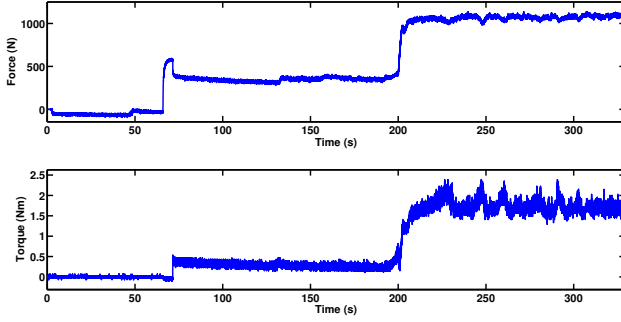


Fig. 5. Illustration of an example of force torque raw data. The top plot shows the thrust force raw data versus time and the bottom plot shows the torque raw data versus time. These raw data covers a whole gun drilling cycle from machine startup to machine shutdown.

TABLE II

DETAILED REAL-WORLD HIGH ASPECT RATIO DEEP HOLE GUN DRILLING EXPERIMENTAL CONDITIONS INCLUDE TOOL DIAMETER, SPINDLE SPEED, FEED RATE AND MACHINING TIME FOR 20 DRILLING INSERTS WITH 6 DIFFERENT TOOL GEOMETRIES.

| Hole Index | Drill Depth (mm) | Tool Geometry | Tool Diameter (mm) | Spindle Speed (rpm) | Feed Rate (um/rev) | Machining Time (s) | Tool Final State |
|------------|------------------|---------------|--------------------|---------------------|--------------------|--------------------|------------------|
| H1-01 | 50 | 1450mm-N4-R9 | 8 | 1200 | 20 | 125.00 | Chipping |
| H1-02 | 50 | | 8 | 1200 | 20 | 125.00 | Broken |
| H2-01 | 50 | 1450mm-N4-R1 | 8 | 800 | 20 | 187.50 | Chipping |
| H2-02 | 50 | | 8 | 800 | 20 | 187.50 | Broken |
| H2-03 | 50 | 1650mm-N8-R1 | 8 | 1650 | 16 | 113.64 | Worn |
| H3-01 | 50 | | 8 | 1650 | 16 | 113.64 | Worn |
| H3-02 | 50 | 1450mm-N8-R9 | 8 | 1650 | 16 | 113.64 | Worn |
| H3-03 | 50 | | 8 | 1650 | 16 | 113.64 | Worn |
| H3-04 | 50 | 1450mm-N8-R9 | 8 | 1650 | 16 | 113.64 | Chipping |
| H3-05 | 50 | | 8 | 1650 | 16 | 113.64 | Chipping |
| H3-06 | 50 | 1650mm-N8-R9 | 8 | 1650 | 16 | 113.64 | Worn |
| H3-07 | 50 | | 8 | 1650 | 16 | 113.64 | Worn |
| H3-08 | 50 | 1650mm-N8-R9 | 8 | 1650 | 16 | 113.64 | Worn |
| H3-09 | 50 | | 8 | 1650 | 16 | 113.64 | Worn |
| H3-10 | 50 | 1650mm-N8-R1 | 8 | 1650 | 16 | 113.64 | Chipping |
| H4-01 | 50 | | 8 | 1650 | 16 | 113.64 | Worn |
| H4-02 | 50 | 1219mm-N8-R9 | 8 | 1650 | 16 | 113.64 | Worn |
| H4-03 | 50 | | 8 | 1650 | 16 | 113.64 | Broken |
| H5-01 | 50 | 1450mm-N8-R9 | 8 | 1650 | 16 | 113.64 | Chipping |
| H5-02 | 50 | | 8 | 1650 | 16 | 113.64 | Chipping |

cycle are as follows.

- 1) Start the machine.
- 2) Feed internal coolant via coolant hole of the gun drill.
- 3) Drill through the workpiece.
- 4) Finish drilling and pull the tool back.
- 5) Shutdown the machine.

The internally-fed coolant exhausts the heat generated during gun drilling process for improved accuracy and precision.

As described in the previous subsection, the data are sent through a DAQ device with various sampling rate for different kinds of sensors. We designed and programmed an automatic data collection and logging system with LabVIEW® (National Instruments, USA) for the purposes of data acquisition, storage and presentation. The sampled signals are acquired, logged and presented on a laptop via data collection and logging system.

C. Data Preprocessing

Data preprocessing includes data alignment, data normalization and time windowing process. The experimental data used in this paper is aligned by the same adaptive Bayesian change point detection (ABCPD) method proposed in [1]. There is no need to give a repetitive introduction of data alignment

TABLE III

DETAILS OF 3 DIFFERENT TYPES OF SENSORS (I.E., ACCELEROMETER, DYNAMOMETER AND MICROSCOPE) USED IN THE GUN DRILLING EXPERIMENTS AND THE OBTAINED MEASUREMENTS INCLUDING VIBRATION, FORCE, TORQUE AND TOOL WEAR.

| Sensor Type | Vibration Sensor | Force and Torque Sensor | Microscope |
|------------------------|---|--|-------------------------------------|
| Description | Kistler 50g 3-axis accelerometer Type 8762A50 | Dynamometer embedded in USK25-2000 machine | Keyence VHX-5000 Digital Microscope |
| # Sensors | 4 | 1 | - |
| # Channels per sensors | 3 | 2 | - |
| Total # Channels | 12 | 2 | - |
| Measurements | Vibration X,Y,Z | Thrust force and torque | Tool wear |
| Frequency (Hz) | 20,000 | 100 | - |

process in this paper. Therefore, only data normalization and time windowing process are introduced in this subsection.

1) *Data Normalization*: In order to handle different ranges of different sensor signals, data normalization is applied on the data to form the normalized inputs in the range of [0,1] prior to any train or test. The normalization is conduct on each sensor signals, this will ensure to treat all sensor signals across all kinds of conditions equally. In another word, the normalization is applied by each dimension of the input data.

2) *Time Windowing Process*: Time windowing process is to move a sliding window along the time axis of multiple sensor signals and map the original data samples into short-time frames. We then extract and select features over the short-time frames.

Suppose τ is the total number of time series data and M is the dimension number of each data sample, the original time series data samples are $\mathbf{X} = (\mathbf{x}_1, \dots, \mathbf{x}_t, \dots, \mathbf{x}_\tau)$, where the t^{th} data sample \mathbf{x}_t is $(x_t^1, \dots, x_t^M)^T$. After time windowing process, we have a series of short-time frames $\hat{\mathbf{X}} = (\hat{\mathbf{x}}_1, \dots, \hat{\mathbf{x}}_t, \dots, \hat{\mathbf{x}}_{\tau-tw})$. The t^{th} data sample $\hat{\mathbf{x}}_t$ becomes $(\mathbf{x}_t, \mathbf{x}_{t+1}, \dots, \mathbf{x}_{t+tw-1})$, where tw denotes the short-time window size. An illustration of time windowing process is shown in Fig. 8.

In general, it is suggested to choose the size of time window equaling to integral multiple of the number of data samples acquired during a full rotation of the spindle or the drive of the machine. The time window size is $tw = N * \frac{60}{S_n * f_s}$, where S_n represents the spindle speed (rpm) and f_s is the sampling frequency (Hz). N denotes the integral multiple. In this paper, the time window size tw is chosen as the number of data samples obtained during one full rotation of the spindle of gun drilling machine (i.e., $N = 1$). Because the gun drilling process is a cyclic rotation process, as the spindle rotates 360 deg, the significant characteristics of the signals repeat.

V. PERFORMANCE EVALUATION METRICS

In this section, the common performance evaluation metrics [1], [4], [10], [11], [23], [30], [39], [40], [43], [45], [57]–[60] for diagnostics and prognostics are reported.

A. Evaluation Metrics for Diagnostics

Considering an imbalance multiclass classification problem, assume y denotes the true target value and \hat{y} represents the estimated target value. \hat{y}_i is the predicted target value of i th data sample \mathbf{x}_i and y_i is the corresponding true target value. N is the total number of data samples. To evaluate the performance

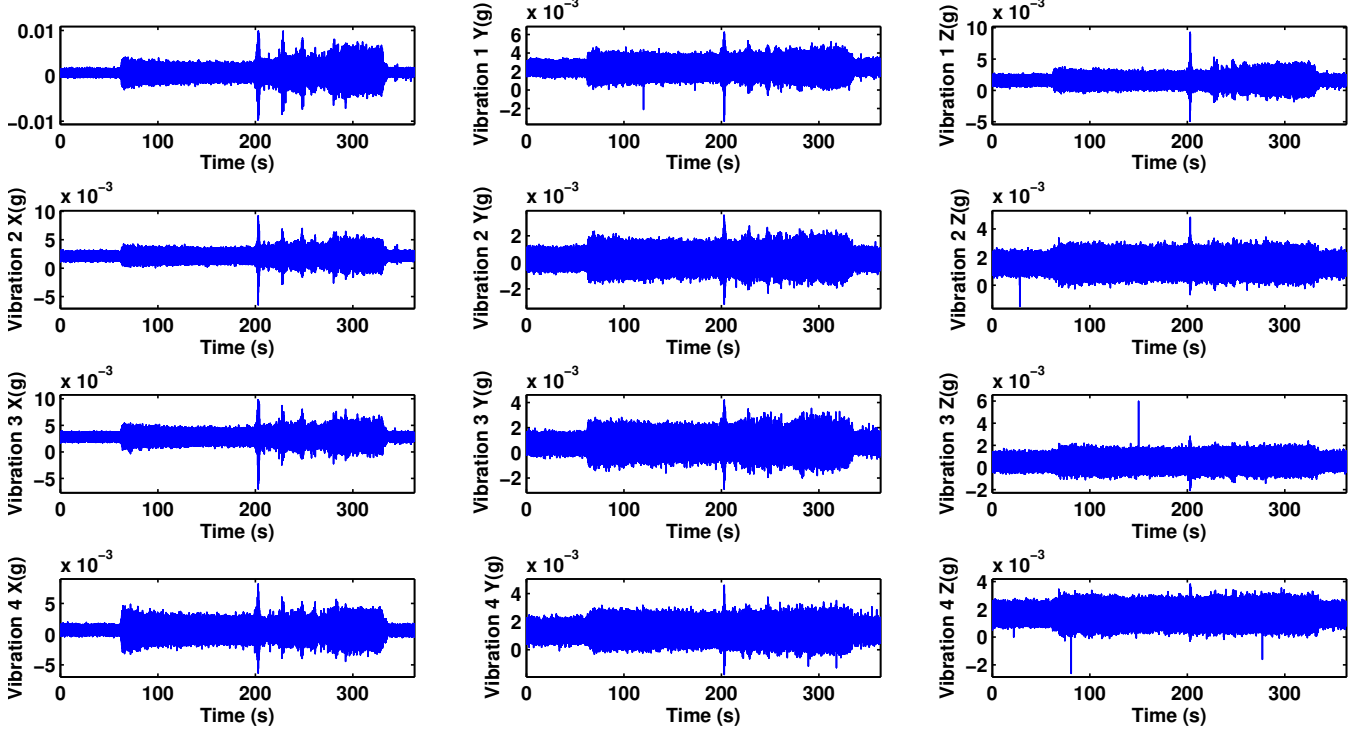


Fig. 6. Illustration of an example of vibration raw data. There are a total of 4 vibration sensors placed on top of the workpiece. Each vibration sensors obtained 3-axis (i.e., x, y, z axes) vibration signals. These raw data cover a whole gun drilling cycle from machine startup to machine shutdown.

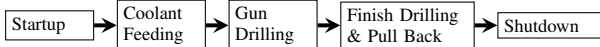


Fig. 7. The procedure of gun drilling experiments includes 5 steps, namely startup, coolant feeding, gun grilling, finish drilling & pull back the drill and finally shutdown the machine.

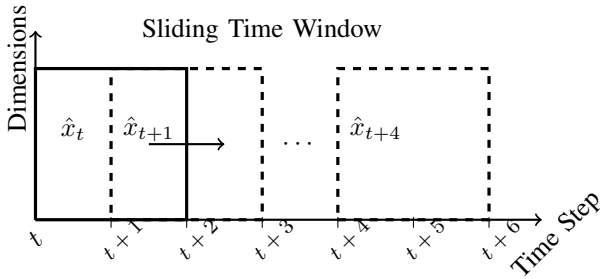


Fig. 8. Illustration of a time windowing process with windowing size of 2 (i.e. $tw = 2$). We obtain short-time frames by moving a sliding window along the time axis of data samples.

of a classifier, the most popular and straightforward evaluation metric is the overall accuracy. The accuracy is formulated as

$$Accuracy = \frac{1}{N} \sum_{i=1}^N 1(\hat{y}_i = y_i), \quad (9)$$

where $1(\cdot)$ is the indicator function.

Unfortunately, in the case of imbalanced data distribution, this measurement does not well describe the performance at

system level [61]. For example, it tends to dilute the actual performance on minority classes.

To provide a balanced view, many other performance metrics were proposed in this research area, such as precision, recall, F1-score and geometric mean (G-mean). In this paper, accuracy, G-mean, precision, recall and F1-score are used. They are formulated in (10) - (13). Note that the weighted average of the G-mean, precision, recall and F1-score of each class are used to evaluate the performance of multiclass classification.

$$G\text{-mean} = \sqrt{\frac{TP}{TP + FN} \times \frac{TN}{TN + FP}}, \quad (10)$$

$$Precision = \frac{TP}{TP + FP}, \quad (11)$$

$$Recall = \frac{TP}{TP + FN}, \quad (12)$$

$$F1\text{-score} = 2 \cdot \frac{precision \times recall}{precision + recall}, \quad (13)$$

where TP, FP, FN, TN represent true positive, false positive, false negative and true negative, respectively.

G-mean evaluates the degree of inductive bias which considers both positive and negative accuracy. The higher G-mean values represent the classifier could handle more balanced and better performance on all classes. G-mean is less sensitive to data distributions. Precision reflects the exactness while recall reflects the detection accuracy. Often times, a system of high precision may lead to low recall, and vice versa. F1-score

represents a balance view between precision and recall in real-world applications.

B. Evaluation Metrics for Prognostics

1) *Root Mean Square Error*: The most popular evaluation metric, i.e., the root mean square error (RMSE) of the estimated tool wear, is used as a performance metric.

$$RMSE = \sqrt{\frac{1}{N} \sum_{i=1}^N (y_i - \hat{y}_i)^2} \quad (14)$$

In this paper, the units of RMSE values are μm .

2) *R2Score*: R2Score is the coefficient of determination of regression score function. The best possible R2Score is 1.0 and it can be negative. A constant model which always predicts the expected value of y , disregarding the input features, would get a R2Score of 0.0. R2Score is an asymmetric function which is defined as (15).

$$R2Score = 1 - \frac{\sum_{i=1}^N (y_i - \hat{y}_i)^2}{\sum_{i=1}^N (y_i - \bar{y})^2} \quad (15)$$

where \bar{y} is the mean of the observations, as $\bar{y} = \frac{1}{N} \sum_{i=1}^N y_i$.

3) *Mean Absolute Percentage Error (MAPE)*: Mean absolute percentage error (MAPE) is a statistical measurement of forecasting prediction accuracy.

$$MAPE = \frac{1}{N} \sum_{i=1}^N \left| \frac{y_i - \hat{y}_i}{y_i} \right| \quad (16)$$

VI. DIAGNOSTICS AND PROGNOSTICS RESULTS

Note that the DBNMS approach consists of both diagnostic and prognostic steps. We would like to evaluate their performance respectively.

A. Implementation Details

In this paper, five-layered ECS-DBN and DBN have been implemented on the gun drilling dataset. The learning rates of both pre-training and fine-tuning are 0.01. The number of pre-training and fine-tuning iterations are 200 and 500 respectively. The range of hidden neuron number is [5, 60]. The hidden neuron number of the networks are randomly selected from the range of hidden neuron number. The dataset is randomly split into training and test datasets. The training ratio is 0.85 and the test ratio is 0.15. All algorithms are trained with 5-fold cross validation. All the simulations have been done for 10 trials.

B. Results of Tool State Estimation

Tool state estimation is also called fault diagnosis in the MDP framework as shown in Fig. 1. It is naturally an imbalanced classification problem. In real-world applications, the fatal faulty cases are always much fewer than healthy cases. Therefore, we form an imbalanced gun drilling dataset and apply ECS-DBN [43] on this dataset to investigate how well the ECS-DBN could handle with imbalanced data on fault diagnosis.

TABLE IV
DETAILS OF THE GUN DRILLING DATASET

| | |
|---------------------------------------|---------------------------|
| Number of Channels | 14 |
| Total Number of Data Samples | 19,712,414 |
| Number of Training Samples | 13,798,690 |
| Number of Testing Samples | 5,913,724 |
| Imbalance Ratio of Class 0 to Class 3 | 1.64 : 1.50 : 1.27 : 1.00 |

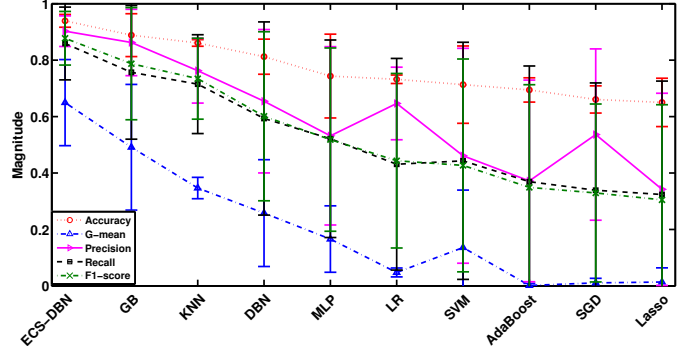


Fig. 9. Illustration of the performance of between different algorithms, i.e., ECS-DBN, Gradient Boosting (GB), K-Nearest Neighbor (KNN), DBN, MLP, Linear Regression (LR), support vector machine (SVM), AdaBoost, SGD and Lasso, on gun drilling imbalanced dataset in terms of accuracy, G-Mean, precision, recall and F1-score.

Table IV summarizes the imbalanced gun drilling dataset. We select the dataset from the raw experimental data by discarding noise data samples. The total number of data samples in the gun drilling dataset is 19,712,414. The number of training data samples and test data samples are 13,798,690 and 5,913,724 respectively. The data are labeled into 4 classes according to Table I. The imbalance ratio (IR) between 4 classes is 1.64:1.50:1.27:1.00.

In the DBN, the number of hidden neurons are randomly chosen from the range of [10, 50]. The activation function of DBN is ReLU. Stochastic gradient descent has been utilized as the fine-tuning training algorithm. The number of pre-training epochs is 300 while the number of fine-tuning epochs is 1000. Training batch size is 500. The parameters of adaptive DE are the same with [43]. We adopt the conventional machine learning algorithms for comparison purpose from [62] with default parameters. In order to show the statistical significance of the performance of ECS-DBN, Wilcoxon paired signed-rank test has been implemented in this section.

The experimental results of imbalanced gun drilling dataset with evolutionary cost-sensitive deep belief network (ECS-DBN), gradient boosting (GB), K-nearest neighbor (KNN), DBN, MLP, linear regression (LR), support vector machine (SVM), AdaBoost, stochastic gradient descent (SGD) and Lasso are shown in Table V in terms of classification accuracy, G-means, Precision, Recall and F1-score. For better illustration, Fig. 9 presents the error bar plot of the performance between different algorithms evaluated with different metrics. All the experimental results include the average performances and the corresponding standard deviation values. The experimental results are obtained on test data. Based on the experimental results, it is obvious that ECS-DBN outperforms other 9 competing algorithms.

TABLE V

COMPARISON OF THE PERFORMANCE BETWEEN EVOLUTIONARY COST-SENSITIVE DEEP BELIEF NETWORK (ECS-DBN) AND DEEP BELIEF NETWORK (DBN), SUPPORT VECTOR MACHINE (SVM), MULTILAYER PERCEPTRON (MLP), K-NEAREST NEIGHBOR CLASSIFIER (KNN), GRADIENT BOOSTING (GB), LOGISTIC REGRESSION (LR), ADABOOST CLASSIFIER, LASSO, AND SGD DIFFERENT MACHINE LEARNING ALGORITHMS ON GUN DRILLING IMBALANCED DATASET IN TERMS OF ACCURACY, G-MEAN, PRECISION, RECALL, F1-SCORE.

| Model Name | Accuracy | G-mean | Precision | Recall | F1-score |
|------------|------------------------|------------------------|------------------------|------------------------|------------------------|
| ECS-DBN | 0.9393 ± 0.0228 | 0.6496 ± 0.1526 | 0.9027 ± 0.0542 | 0.8591 ± 0.1289 | 0.8776 ± 0.0950 |
| GB | 0.8886 ± 0.0760 | 0.4913 ± 0.2227† | 0.8626 ± 0.1177 | 0.7568 ± 0.2368† | 0.7875 ± 0.1988† |
| KNN | 0.8609 ± 0.0117† | 0.3468 ± 0.0378† | 0.7626 ± 0.1147† | 0.7150 ± 0.1751† | 0.7343 ± 0.1435† |
| DBN | 0.8123 ± 0.0623† | 0.2581 ± 0.1892† | 0.6543 ± 0.2541† | 0.5933 ± 0.3422† | 0.6012 ± 0.2996† |
| MLP | 0.7435 ± 0.1485† | 0.1660 ± 0.1177† | 0.5319 ± 0.3160 | 0.5215 ± 0.3499† | 0.5184 ± 0.3249† |
| LR | 0.7322 ± 0.0150† | 0.0476 ± 0.0157† | 0.6465 ± 0.1286† | 0.4311 ± 0.3751† | 0.4436 ± 0.3093† |
| SVM | 0.7132 ± 0.1371† | 0.1359 ± 0.2037† | 0.4612 ± 0.3808† | 0.4433 ± 0.4201† | 0.4270 ± 0.3772† |
| AdaBoost | 0.6944 ± 0.0429† | 0.0017 ± 0.0073† | 0.3721 ± 0.3574† | 0.3693 ± 0.4100† | 0.3491 ± 0.3639† |
| SGD | 0.6607 ± 0.0481† | 0.0107 ± 0.0163† | 0.5363 ± 0.3036† | 0.3390 ± 0.3802† | 0.3294 ± 0.3153† |
| Lasso | 0.6503 ± 0.0858† | 0.0139 ± 0.0502† | 0.3422 ± 0.3406† | 0.3238 ± 0.4021† | 0.3049 ± 0.3373† |

† indicates that the difference between marked algorithm and the proposed algorithm is statistically significant using Wilcoxon rank sum test at the 5% significance level.

TABLE VI

COMPARISON OF THE AVERAGE COMPUTATIONAL TIME OF ECS-DBN AND DBN WITH 5-FOLD CROSS VALIDATION ON THE GUN DRILLING IMBALANCED DATASET OVER 10 TRIALS.

| Model Name | Average Computational Time(s) | Average Computational Time without DBN training time(s) |
|------------|-------------------------------|---|
| ECS-DBN | 9977.39 ± 148.55 | 1280.28 |
| DBN | 8697.11 ± 2308.22 | - |

1) *Suitability*: We report the accuracy via a 5-fold cross validation over 10 trials in Table V. ECS-DBN outperforms all other competing algorithms. The results suggest that ECS-DBN is more suitable for diagnostics than the other competing algorithms, therefore, potentially leads to better prognostics in the MDP framework.

2) *Stability*: To measure the stability of the diagnostics module, the performance variance are compared. It is noted in Table V that, ECS-DBN outperforms other competing algorithms with comparably lower variances. This suggests that ECS-DBN could provide lesser variance in predictions so as to enhance the stability of the diagnostic module.

3) *Quality*: For quality evaluation of the classification made by diagnostic module, F1-score is calculated [60]. F1-score represents the trade-off between precision and recall by interpreting a harmonic mean between precision and recall. Higher F1-score represents better quality of predictions. According to Table V, we observe that ECS-DBN achieves the best average F1-score over 10 trials of 0.8776 with a low variance of 0.0950 among other competing algorithms. The performance of the ECS-DBN suggests that it could provide quite good quality of diagnostic predictions.

4) *Computational Time Analysis*: Average computational time of ECS-DBN and DBN are presented in Table VI. Based on the computational time without DBN training time, it can be observed that comparing with the training time of DBN, the average time of adjusting proper misclassification costs by evolutionary algorithm is very small that can be ignored. Therefore, ECS-DBN with evolutionary algorithm to find the appropriate misclassification costs is quite efficient for imbalanced multiclass classification and thus makes ECS-DBN to be applicable in diagnostic module.

C. Results of Tool Wear Estimation

Tool wear estimation is the prognostic step in the MDP framework as shown in Fig. 1. In this section, the analysis of the results mainly consists of three parts. Firstly, we evaluate its performance under different signal states. Secondly, the performance of DBNMS approach is evaluated and compared with other single state approaches at algorithmic level. Finally, the comparison between MDP framework and other single state frameworks at system level is presented.

1) *Comparison of Different Signal States*: Sensor selection is an important part in numerous industry applications which is widely used to reduce costs and easy installation. To verify the effects of different signal states, the simulations of DBNMS with the signals from different kinds of sensors have been carried out in this section. In this real-world experiment two kinds of sensors have been used, namely dynamometer and accelerometer. The force and torque signals are taken from the same dynamometer while 12 vibration signals are obtained from 4 accelerometers. Therefore, totally 7 different combinations of sensor signals including single force signal, single torque signal, 12 vibration signals from accelerometers, force and torque signals (F-T), force and vibration signals (F-Vib), torque and vibration signals (T-Vib), all force, torque and vibration signals from both dynamometer and accelerometers (F-T-Vib) have been investigated in this section.

Table VII shows the test results of DBNMS with 7 different combinations of sensor signals, i.e., force, torque, vibration, force and torque (F-T), force and vibration (F-Vib), torque and vibration (T-Vib), all force, torque and vibration signals (F-T-Vib). The performance of DBNMS are divided into two parts with and without smoothing the outputs. DBNMS (smooth) represents a DBNMS with a moving average smoothing applied on the regression outputs. It is obvious that the DBNMS with F-T-Vib outperforms other six combinations of sensor inputs (i.e., force, torque, vibration, F-T, F-Vib, T-Vib), in terms of RMSE, R2Score, MAPE. By comparing the performances between DBNMS and DBNMS (smooth), we note that smoothing has improved the performance. Since the tool wear increases with time, the smoothed estimation outputs are more reasonable and suitable for this application.

For better illustration, the results of DBNMS and DBNMS

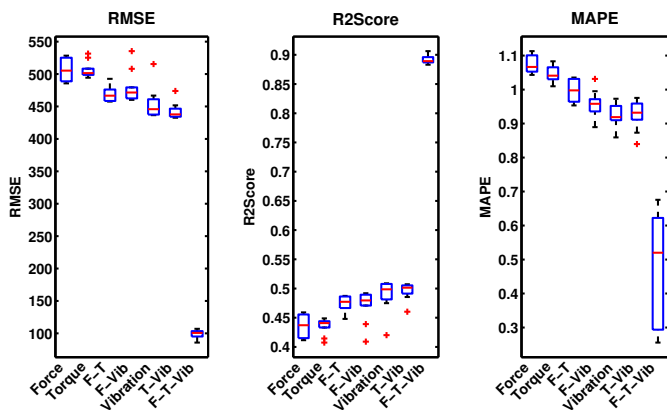


Fig. 10. Illustration of the comparison between the overall performance of DBNMS with 7 different combinations of sensor inputs, i.e., torque, force, force and torque (F-T), vibration, force and vibration (F-Vib), torque and vibration (T-Vib), all force, torque and vibration signals (F-T-Vib), on test data with all sensor inputs over 10 trials in terms of RMSE, R2Score and MAPE, respectively. The boxplot shows the minimum, median and maximum values of different metrics obtained over 10 trials without smoothing.

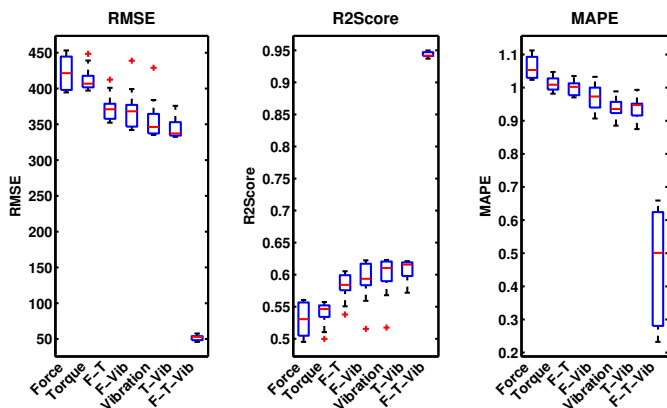


Fig. 11. Illustration of the comparison between the overall performance of DBNMS (smooth) with 7 different combinations of sensor inputs, i.e., torque, force, force and torque (F-T), vibration, force and vibration (F-Vib), torque and vibration (T-Vib), all force, torque and vibration signals (F-T-Vib), on test data with all sensor inputs over 10 trials in terms of RMSE, R2Score and MAPE, respectively. The boxplot shows the minimum, median and maximum values of different metrics obtained over 10 trials with smoothing.

(smooth) are also summarized and shown in Fig. 10 and Fig. 11, respectively. According to the figures, it is clear that the combination of F-T-Vib obtained lower average RMSE values, lower average MAPE values and higher average R2Score values with small variance than other six combinations. The results also show that we benefit from the fusion of multiple sensing signals. Therefore, in the rest of the paper, all force, torque, vibration signals are used as the inputs.

2) *Comparison of Different Algorithms:* In order to study the effects of multi-state approach and single state approach at algorithmic level, 12 different regression algorithms, i.e., DBNMS (smooth), DBNMS, DBN, MLP, extreme learning machine (ELM), support vector machine (SVM), ridge regression (RR), Lasso, AdaBoost regressor (AdaBoost), stochastic gradient descent regressor (SGD), elastic net (EN) and least angle regression (LAR), have been implemented with the same data inputs (i.e., preprocessed raw data without feature ex-

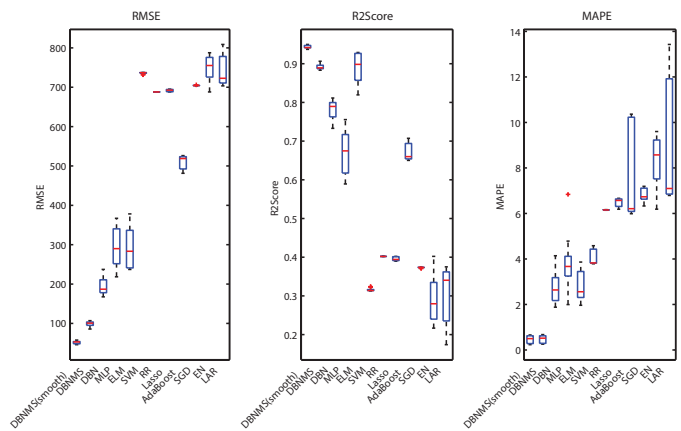


Fig. 12. Illustration of the comparison between the overall performance of DBNMS and DBNMS (smooth) with 10 different algorithms, i.e., DBN, multilayer perceptron (MLP), extreme learning machine (ELM), support vector machine (SVM), ridge regression (RR), Lasso, AdaBoost, stochastic gradient descent regressor (SGD), elastic net (EN), least angle regression (LAR), on test data with all sensor inputs over 10 trials in terms of RMSE, R2Score and MAPE, respectively.

traction/selection). ELM is a single hidden layer feed-forward neural network with randomized connection weights between the input and hidden layers and analytically determined connection weights between the hidden and output layers [63]. SVM [64] is one of the most popular supervised learning techniques which constructs a class separation hyper-plane in a high-dimensional space implicitly defined via a certain kernel function. RR [65] is a linear least square regression with l_2 regularization. LASSO [66] is a linear regression model with an l_1 regularizer. AdaBoost [67] is a meta-estimator by fitting an ensemble to the dataset while adjusting the ensemble weights according to the current errors. SGD [68] is using an efficient stochastic gradient descent learning approach to fit convex loss functions to fit linear regression models. EN [69] is a linear regression with combined l_1 and l_2 regularizer. LAR [70] is a kind of forward stepwise regression algorithm to find predictors who are most correlated with the targets.

The experimental results of these 12 different algorithms are obtained on test data. Their performances on test data with all sensor inputs over 10 trials are shown in Table VIII in terms of RMSE, R2Score and MAPE. From the observation in Table VIII, DBNMS has shown lower average RMSE values, lower average MAPE values and higher R2Score values than those of other competing algorithms. Thus, the results indicate that DBNMS has better average performance with low variance than many popular algorithms. To clearly illustrate the comparison results between different algorithms, the results are plotted into three boxplots in terms of RMSE, R2Score, MAPE respectively in Fig. 12. It is obvious that DBNMS outperforms other algorithms in terms of RMSE, R2Score and MAPE.

3) *Computational Time Analysis:* Table IX reports the average computational time of 11 different regression algorithms, i.e., DBNMS, DBN, GB, ELM, SVM, RR, Lasso, AdaBoost, SGD, EN and LAR over 10 runs on gun drilling dataset with time windowing processing. It can be observed that LAR

TABLE VII

COMPARISON OF THE TEST PERFORMANCES OBTAINED BY DBNMSs WITH 7 DIFFERENT COMBINATIONS OF SENSOR INPUTS, I.E., FORCE, TORQUE, VIBRATION, FORCE AND TORQUE (F-T), FORCE AND VIBRATION (F-VIB), TORQUE AND VIBRATION (T-VIB), ALL FORCE, TORQUE AND VIBRATION SIGNALS (F-T-VIB) IN TERMS OF RMSE, R2SCORE AND MAPE OVER 10 RUNS WITH SMOOTHING AND WITHOUT SMOOTHING.

| Signal States | Without Smoothing | | | With Smoothing | | |
|-------------------------------|-----------------------|----------------------|----------------------|-----------------------|----------------------|----------------------|
| | RMSE | R2Score | MAPE | RMSE | R2Score | MAPE |
| force | 506.9173 ± 17.86 | 0.4355 ± 0.02 | 1.0742 ± 0.03 | 422.2615 ± 23.67 | 0.5297 ± 0.03 | 1.0600 ± 0.03 |
| torque | 505.8085 ± 12.64 | 0.4361 ± 0.01 | 1.0438 ± 0.03 | 413.0445 ± 17.27 | 0.5395 ± 0.02 | 1.0114 ± 0.02 |
| vibration | 454.2334 ± 24.38 | 0.4891 ± 0.03 | 0.9221 ± 0.04 | 357.3197 ± 29.49 | 0.5981 ± 0.03 | 0.9395 ± 0.03 |
| force-torque | 469.5890 ± 12.24 | 0.4739 ± 0.01 | 0.9971 ± 0.03 | 373.7561 ± 19.65 | 0.5812 ± 0.02 | 0.9999 ± 0.02 |
| force-vibration | 479.1852 ± 24.39 | 0.4710 ± 0.03 | 0.9556 ± 0.04 | 371.9768 ± 29.46 | 0.5894 ± 0.03 | 0.9732 ± 0.04 |
| torque-vibration | 442.3175 ± 12.66 | 0.4962 ± 0.01 | 0.9250 ± 0.04 | 344.4068 ± 15.28 | 0.6077 ± 0.02 | 0.9369 ± 0.04 |
| force-torque-vibration | 99.3405 ± 6.22 | 0.8913 ± 0.01 | 0.4661 ± 0.17 | 52.0264 ± 3.55 | 0.9431 ± 0.00 | 0.4545 ± 0.18 |

TABLE VIII

COMPARISON OF THE AVERAGE PERFORMANCE BETWEEN DBNMS, DBNMS (SMOOTH) AND OTHER COMPETING ALGORITHMS, I.E., DEEP BELIEF NETWORK (DBN), MULTILAYER PERCEPTION (MLP), EXTREME LEARNING MACHINE (ELM), SUPPORT VECTOR MACHINE (SVM), RIDGE REGRESSION (RR), LASSO, ADABOOST, STOCHASTIC GRADIENT DESCENT REGRESSOR (SGD), ELASTIC NET (EN), LEAST ANGLE REGRESSION (LAR), ON TEST DATA WITH ALL SENSOR INPUTS OVER 10 TRIALS.

| Models | RMSE | R2Score | MAPE |
|-----------------------|-----------------------|----------------------|----------------------|
| DBNMS (smooth) | 52.0264 ± 3.55 | 0.9431 ± 0.00 | 0.4545 ± 0.18 |
| DBNMS | 99.3405 ± 6.22 | 0.8913 ± 0.01 | 0.4661 ± 0.17 |
| DBN | 198.3531 ± 23.95 | 0.7767 ± 0.03 | 2.8829 ± 0.69 |
| MLP | 290.8781 ± 52.07 | 0.6739 ± 0.06 | 3.8347 ± 1.32 |
| ELM | 291.2265 ± 52.14 | 0.8098 ± 0.04 | 2.7823 ± 0.67 |
| SVM | 736.0593 ± 2.21 | 0.3158 ± 0.00 | 4.0392 ± 0.34 |
| RR | 688.0910 ± 0.00 | 0.4021 ± 0.00 | 6.1551 ± 0.01 |
| Lasso | 691.8248 ± 2.84 | 0.3955 ± 0.00 | 6.4928 ± 0.18 |
| AdaBoost | 511.3269 ± 16.91 | 0.6695 ± 0.02 | 7.7717 ± 2.15 |
| SGD | 704.4564 ± 0.59 | 0.3733 ± 0.00 | 6.8171 ± 0.30 |
| EN | 748.8569 ± 32.58 | 0.2906 ± 0.06 | 8.3298 ± 1.10 |
| LAR | 741.2134 ± 40.93 | 0.3043 ± 0.08 | 8.9735 ± 2.84 |

TABLE IX

THE AVERAGE COMPUTATIONAL TIME OF DIFFERENT ALGORITHMS (I.E., DBNMS, DBN, MLP, ELM, SVM, RR, LASSO, ADABOOST, SGD, EN, LAR) OVER 10 TRIALS.

| Models | Computational Time (s) |
|----------|------------------------|
| DBNMS | 6,296.26 ± 1,533.75 |
| DBN | 1,754.89 ± 1,158.67 |
| MLP | 59.30 ± 34.28 |
| ELM | 1.89 ± 1.45 |
| SVM | 95.68 ± 1.50 |
| RR | 0.03 ± 0.01 |
| Lasso | 0.59 ± 0.22 |
| AdaBoost | 7.24 ± 5.18 |
| SGD | 0.12 ± 0.02 |
| EN | 0.24 ± 0.28 |
| LAR | 0.02 ± 0.01 |

has the shortest average running time. DBNMS is still useful for TCM with more accurate performance in spite of longer training time. Our experimental platform is a desktop PC with Intel Core i7-3770 3.40GHz CPU, NVIDIA GeForce GTX 980 and 32GB RAM. All the simulations are done under Linux system.

4) *Comparison of Different Frameworks:* To evaluate the frameworks as shown in Fig. 1 at system level, namely, conventional data-driven based, deep learning based and MDP, we summarize the performance of these frameworks in Table. X. Since there is a lack of physical model for these specific gun drills, we do not compare MDP with physical-based

TABLE X

COMPARISON OF THE AVERAGE PERFORMANCE BETWEEN MDP, MDP (WITH SMOOTHING) AND OTHER FRAMEWORK, I.E., DEEP LEARNING BASED FRAMEWORK, CONVENTIONAL DATA-DRIVEN FRAMEWORK ON TEST DATA. MDP OUTPERFORMS OTHER COMPETING FRAMEWORKS.

| Models | RMSE | R2Score |
|--|-----------------------|----------------------|
| MDP (smooth) | 52.0264 ± 3.55 | 0.9431 ± 0.00 |
| MDP | 99.3405 ± 6.22 | 0.8913 ± 0.01 |
| Conventional data-driven framework (MLP-PCC) [1] | 118.7091 ± 9.20 | 0.8666 ± 0.01 |
| Deep learning based framework (DBN) | 198.3531 ± 23.95 | 0.7767 ± 0.03 |

framework in this paper. Here the MLP-PCC [1] is chosen to represent the conventional data-driven framework. A DBN based framework with automatic feature learning is a typical deep learning approach solution. To show the effect of multi-state modeling, we only implement the multi-state in MDP framework, and single state in both conventional and deep learning framework.

From Table. X, it is observed that the proposed MDP outperforms conventional data-driven based framework as well as deep learning based framework in terms of RMSE and R2Score. With multi-state modeling, MDP can provide more accurate results than other single state frameworks.

VII. CONCLUSION

In this paper, a multi-state diagnosis and prognosis (MDP) framework has been proposed for tool condition monitoring using a deep belief network based multi-state approach (DBNMS). The proposed DBNMS is based on the multiple tool states identified by ECS-DBN that can switch to appropriate prognostic degradation models for prediction. The DBNMS has been applied to tool wear prediction on gun drilling and the experimental studies show that the DBNMS outperforms many popular machine learning algorithms in tool condition monitoring. It has also been shown that the DBNMS is able to generate more accurate and robust prognostic predictions and has good generalization ability over various operating conditions.

To elevate the overall performance of TCM, diagnosis and prognosis are tied in one framework. Due to different data attributes in different health states, a multi-state diagnosis and prognosis framework has been proposed. The proposed MDP framework is one step further towards an unified end-to-end diagnosis and prognosis framework for TCM.

We hope to extend the idea to other conventional data-driven frameworks. Our future work includes the application of multi-

objective deep belief networks ensemble (MODBNE) [4] as the degradation model to obtain optimal hyper-parameters for better performance. Other deep learning architectures will also be examined based on the gun drilling real-world experimental datasets to achieve better accuracy in TCM.

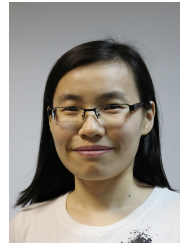
ACKNOWLEDGMENT

This work was done with the help from NUS Mechanical Engineering department and SIMTech. Thanks for the helps in mechanical experiments from Dennis Neo Wee Keong, Malarvizhi Sankaranarayananasamy, Lew Maan Tarng, Dr. Liu Kui, Dr. Woon Ken Soon, Md Tanjilul Islam, Afiq and all the other members from the NUS-SIMTech Joint Lab.

REFERENCES

- [1] C. Zhang, G. S. Hong, H. Xu, K. C. Tan, J. H. Zhou, H. L. Chan, and H. Li, "A data-driven prognostics framework for tool remaining useful life estimation in tool condition monitoring," in *IEEE Int. Conf. Emerg. (ETFA), 2017*. IEEE, Sept 2017, pp. 1–8.
- [2] J. Hong, J. Zhou, H. L. Chan, C. Zhang, H. Xu, and G. S. Hong, "Tool condition monitoring in deep hole gun drilling: a data-driven approach," in *IEEE Int. Conf. Ind. Eng. Eng. Manage. (IEEM), 2017*. IEEE, Dec 2017, pp. 2148–2152.
- [3] G. Hinton, S. Osindero, and Y.-W. Teh, "A fast learning algorithm for deep belief nets," *Neural Comput.*, vol. 18, no. 7, pp. 1527–1554, 2006.
- [4] C. Zhang, P. Lim, A. K. Qin, and K. C. Tan, "Multiobjective deep belief networks ensemble for remaining useful life estimation in prognostics," *IEEE T. Neur. Net. Lear.*, vol. 28, no. 10, pp. 2306–2318, Oct 2017.
- [5] M. Wang and J. Wang, "Chmm for tool condition monitoring and remaining useful life prediction," *Int. J. Adv. Manu. Tech.*, vol. 59, no. 5, pp. 463–471, 2012.
- [6] C. H. R. Martins, P. R. Aguiar, A. Frech, and E. C. Bianchi, "Tool condition monitoring of single-point dresser using acoustic emission and neural networks models," *IEEE Trans. Instrument. Measure.*, vol. 63, no. 3, pp. 667–679, March 2014.
- [7] Y. Liu, Q. Shuai, S. Zhou, and J. Tang, "Prognosis of structural damage growth via integration of physical model prediction and bayesian estimation," *IEEE T. Reliab.*, vol. PP, no. 99, pp. 1–12, 2017.
- [8] K. Zhu, Y. San Wong, and G. S. Hong, "Wavelet analysis of sensor signals for tool condition monitoring: A review and some new results," *Inter. J. Machine Tools Manuf.*, vol. 49, no. 7, pp. 537–553, 2009.
- [9] J. Sun, G. Hong, M. Rahman, and Y. Wong, "Identification of feature set for effective tool condition monitoring by acoustic emission sensing," *Inter. J. Prod. Res.*, vol. 42, no. 5, pp. 901–918, 2004.
- [10] G. Hong, M. Rahman, and Q. Zhou, "Using neural network for tool condition monitoring based on wavelet decomposition," *Inter. J. Machine Tools Manuf.*, vol. 36, no. 5, pp. 551–566, 1996.
- [11] H. Xu, C. Zhang, G. S. Hong, J. H. Zhou, J. Hong, and K. S. Woon, "Gated recurrent units based neural network for tool condition monitoring," in *IEEE Int. Joint Conf. Neural Netw. (IJCNN), 2018, accepted*. IEEE, July 2018.
- [12] J. Sun, M. Rahman, Y. Wong, and G. Hong, "Multiclassification of tool wear with support vector machine by manufacturing loss consideration," *Inter. J. Machine Tools Manuf.*, vol. 44, no. 11, pp. 1179–1187, 2004.
- [13] A. Widodo and B.-S. Yang, "Support vector machine in machine condition monitoring and fault diagnosis," *Mech. Syst. Signal Process.*, vol. 21, no. 6, pp. 2560–2574, 2007.
- [14] X. Li, S. K. Tso, and J. Wang, "Real-time tool condition monitoring using wavelet transforms and fuzzy techniques," *IEEE T. Syst. Man Cy. C*, vol. 30, no. 3, pp. 352–357, 2000.
- [15] X. Li, H.-X. Li, X.-P. Guan, and R. Du, "Fuzzy estimation of feed-cutting force from current measurement—a case study on intelligent tool wear condition monitoring," *IEEE T. Syst. Man Cy. C*, vol. 34, no. 4, pp. 506–512, 2004.
- [16] P. Fu and A. Hope, "A hybrid pattern recognition architecture for cutting tool condition monitoring," in *Pattern Recognition Techniques, Technology and Applications*. InTech, 2008.
- [17] J. Liu, Y. Hu, B. Wu, and C. Jin, "A hybrid health condition monitoring method in milling operations," *The International Journal of Advanced Manufacturing Technology*, pp. 1–12, 2017.
- [18] I. Tansel, M. Trujillo, A. Nedbouyan, C. Velez, W.-Y. Bao, T. Arkan, and B. Tansel, "Micro-end-milling-III. wear estimation and tool breakage detection using acoustic emission signals," *Inter. J. Machine Tools Manuf.*, vol. 38, no. 12, pp. 1449–1466, 1998.
- [19] D. Shi and N. N. Gindy, "Industrial applications of online machining process monitoring system," *IEEE/ASME Trans. Mechatronics*, vol. 12, no. 5, pp. 561–564, 2007.
- [20] K. Zhu, Y. Wong, and G. Hong, "Multi-category micro-milling tool wear monitoring with continuous hidden markov models," *Mech. Syst. Signal Process.*, vol. 23, no. 2, pp. 547–560, 2009.
- [21] J.-H. Zhou, C. K. Pang, Z.-W. Zhong, and F. L. Lewis, "Tool wear monitoring using acoustic emissions by dominant-feature identification," *IEEE T. Instrum. Meas.*, vol. 60, no. 2, pp. 547–559, 2011.
- [22] W.-H. Hsieh, M.-C. Lu, and S.-J. Chiou, "Application of backpropagation neural network for spindle vibration-based tool wear monitoring in micro-milling," *Inter. J. Adv. Manuf. Technol.*, vol. 61, no. 1, pp. 53–61, 2012.
- [23] O. Geramifard, J.-X. Xu, J.-H. Zhou, and X. Li, "A physically segmented hidden markov model approach for continuous tool condition monitoring: Diagnostics and prognostics," *IEEE T. Ind. Inform.*, vol. 8, no. 4, pp. 964–973, 2012.
- [24] J. M. Karandikar, A. E. Abbas, and T. L. Schmitz, "Tool life prediction using bayesian updating. part 1: Milling tool life model using a discrete grid method," *Precis. Eng.*, vol. 38, no. 1, pp. 9–17, 2014.
- [25] F. Camci and R. B. Chinnam, "Health-state estimation and prognostics in machining processes," *IEEE Trans. Autom. Sci. Eng.*, vol. 7, no. 3, pp. 581–597, 2010.
- [26] X. Li, A. Djordjevich, and P. K. Venuninod, "Current-sensor-based feed cutting force intelligent estimation and tool wear condition monitoring," *IEEE T. Ind. Electron.*, vol. 47, no. 3, pp. 697–702, 2000.
- [27] V. Venkatasubramanian, R. Rengaswamy, K. Yin, and S. N. Kavuri, "A review of process fault detection and diagnosis: Part i: Quantitative model-based methods," *Comput. Chem. Eng.*, vol. 27, no. 3, pp. 293–311, 2003.
- [28] K. Zhu, T. Mei, and D. Ye, "Online condition monitoring in micro-milling: A force waveform shape analysis approach," *IEEE T. Ind. Electron.*, vol. 62, no. 6, pp. 3806–3813, June 2015.
- [29] K. Zhu, Y. San Wong, and G. S. Hong, "Multi-category micro-milling tool wear monitoring with continuous hidden markov models," *Mech. Syst. Signal Process.*, vol. 23, no. 2, pp. 547–560, 2009.
- [30] O. Geramifard, J.-X. Xu, J.-H. Zhou, and X. Li, "Multimodal hidden markov model-based approach for tool wear monitoring," *IEEE T. Ind. Electron.*, vol. 61, no. 6, pp. 2900–2911, 2014.
- [31] W. Yue, Y. Wong, and G. S. Hong, "Adaptive-vdmm for prognostics in tool condition monitoring," in *Int. Conf. Autom., Robot. Appl. (ICRA), 2015*. IEEE, 2015, pp. 131–136.
- [32] K. Zhu and T. Liu, "On-line tool wear monitoring via hidden semi-markov model with dependent durations," *IEEE T. Ind. Inform.*, vol. PP, no. 99, pp. 1–1, 2017.
- [33] A. Soualhi, G. Clerc, H. Razik, F. Guillet *et al.*, "Hidden markov models for the prediction of impending faults," *IEEE T. Ind. Electron.*, vol. 63, no. 5, pp. 3271–3281, 2016.
- [34] W. Li, S. Zhang, and S. Rakheja, "Feature denoising and nearest-farthest distance preserving projection for machine fault diagnosis," *IEEE T. Ind. Inform.*, vol. 12, no. 1, pp. 393–404, 2016.
- [35] Z. Du, X. Chen, H. Zhang, and R. Yan, "Sparse feature identification based on union of redundant dictionary for wind turbine gearbox fault diagnosis," *IEEE T. Ind. Electron.*, vol. 62, no. 10, pp. 6594–6605, 2015.
- [36] A. Soualhi, H. Razik, G. Clerc, and D. D. Doan, "Prognosis of bearing failures using hidden markov models and the adaptive neuro-fuzzy inference system," *IEEE T. Ind. Electron.*, vol. 61, no. 6, pp. 2864–2874, 2014.
- [37] C.-M. Vong, P.-K. Wong, and W.-F. Ip, "A new framework of simultaneous-fault diagnosis using pairwise probabilistic multi-label classification for time-dependent patterns," *IEEE T. Ind. Electron.*, vol. 60, no. 8, pp. 3372–3385, 2013.
- [38] X. Jin, M. Zhao, T. W. Chow, and M. Pecht, "Motor bearing fault diagnosis using trace ratio linear discriminant analysis," *IEEE T. Ind. Electron.*, vol. 61, no. 5, pp. 2441–2451, 2014.
- [39] P. Lim, C. K. Goh, K. C. Tan, and P. Dutta, "Multimodal degradation prognostics based on switching kalman filter ensemble," *IEEE T. Neur. Net. Lear.*, vol. 28, no. 1, pp. 136–148, Jan 2017.
- [40] P. Lim, C. Goh, K. Tan, and P. Dutta, "Estimation of remaining useful life based on switching kalman filter neural network ensemble," 2014, pp. 2–9.

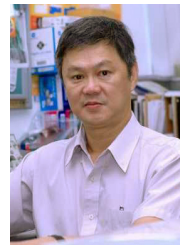
- [41] L. Liao, "Discovering prognostic features using genetic programming in remaining useful life prediction," *IEEE T. Ind. Electron.*, vol. 61, no. 5, pp. 2464–2472, 2014.
- [42] X. Li, R. Du, B. Denkena, and J. Imiela, "Tool breakage monitoring using motor current signals for machine tools with linear motors," *IEEE T. Ind. Electron.*, vol. 52, no. 5, pp. 1403–1408, 2005.
- [43] C. Zhang, K. C. Tan, H. Li, and G. S. Hong, "A cost-sensitive deep belief network for imbalanced classification," *IEEE T. Neur. Net. Lear.*, 2018.
- [44] —, "A cost-sensitive deep belief network for imbalanced classification," *arXiv preprint arXiv:2243077*, 2018.
- [45] C. Zhang, K. C. Tan, and R. Ren, "Training cost-sensitive deep belief networks on imbalance data problems," in *IEEE Int. Joint Conf. Neural Netw. (IJCNN)*, 2016. IEEE, July 2016, pp. 4362–4367.
- [46] J. O. Berger, *Statistical decision theory and Bayesian analysis*. Springer Science & Business Media, 2013.
- [47] C. Elkan, "The foundations of cost-sensitive learning," in *Int. Joint Conf. Artif. Intell.*, vol. 17, no. 1. Citeseer, 2001, pp. 973–978.
- [48] M. Kukar, I. Kononenko *et al.*, "Cost-sensitive learning with neural networks," in *ECAI*. Citeseer, 1998, pp. 445–449.
- [49] J. Zhang and A. C. Sanderson, "Jade: adaptive differential evolution with optional external archive," *IEEE T. Evolut. Comput.*, vol. 13, no. 5, pp. 945–958, 2009.
- [50] A. K. Qin and P. N. Suganthan, "Self-adaptive differential evolution algorithm for numerical optimization," in *IEEE Congr. Evolut. Comput.*, 2005, vol. 2. IEEE, 2005, pp. 1785–1791.
- [51] A. K. Qin, V. L. Huang, and P. N. Suganthan, "Differential evolution algorithm with strategy adaptation for global numerical optimization," *IEEE T. Evolut. Comput.*, vol. 13, no. 2, pp. 398–417, 2009.
- [52] P. Lim, C. K. Goh, and K. C. Tan, "A time window neural network based framework for remaining useful life estimation," in *Neur. Net. (IJCNN)*, 2016 *Int. Joint Conf.* IEEE, 2016, pp. 1746–1753.
- [53] T. Benkedjouh, K. Medjaher, N. Zerhouni, and S. Rechak, "Remaining useful life estimation based on nonlinear feature reduction and support vector regression," *Eng. Appl. Artif. Intell.*, vol. 26, no. 7, pp. 1751–1760, 2013.
- [54] H.-Z. Huang, H.-K. Wang, Y.-F. Li, L. Zhang, and Z. Liu, "Support vector machine based estimation of remaining useful life: current research status and future trends," *J. Mech. Sci. Tech.*, vol. 29, no. 1, pp. 151–163, 2015.
- [55] G. Hinton, "A practical guide to training restricted boltzmann machines," *Momentum*, vol. 9, no. 1, p. 926, 2010.
- [56] Y. Bengio, P. Lamblin, D. Popovici, H. Larochelle *et al.*, "Greedy layer-wise training of deep networks," *Adv. Neural Info. Process. Syst.*, vol. 19, p. 153, 2007.
- [57] J. Wang, J. Xie, R. Zhao, K. Mao, and L. Zhang, "A new probabilistic kernel factor analysis for multisensory data fusion: application to tool condition monitoring," *IEEE T. Instrum. Meas.*, vol. 65, no. 11, pp. 2527–2537, 2016.
- [58] C. Zhang, X. Yao, J. Zhang, and H. Jin, "Tool condition monitoring and remaining useful life prognostic based on a wireless sensor in dry milling operations," *Sensors*, vol. 16, no. 6, p. 795, 2016.
- [59] C. Zhang, J. H. Sun, and K. C. Tan, "Deep belief networks ensemble with multi-objective optimization for failure diagnosis," in *IEEE Int. Conf. Syst. Man Cyb. (SMC)*, 2015. IEEE, 2015.
- [60] A. K. Jain and B. K. Lad, "A novel integrated tool condition monitoring system," *Journal of Intelligent Manufacturing*, pp. 1–14, 2017.
- [61] H. He, E. Garcia *et al.*, "Learning from imbalanced data," *IEEE T. Knowl. Data En.*, vol. 21, no. 9, pp. 1263–1284, 2009.
- [62] F. Pedregosa, G. Varoquaux, A. Gramfort, V. Michel, B. Thirion, O. Grisel, M. Blondel, P. Prettenhofer, R. Weiss, V. Dubourg, J. Vanderplas, A. Passos, D. Cournapeau, M. Brucher, M. Perrot, and E. Duchesnay, "Scikit-learn: Machine learning in Python," *J. Mach. Learn. Res.*, vol. 12, pp. 2825–2830, 2011.
- [63] G.-B. Huang, Q.-Y. Zhu, and C.-K. Siew, "Extreme learning machine: theory and applications," *Neurocomputing*, vol. 70, no. 1, pp. 489–501, 2006.
- [64] B. S. Alex J Smola, "A tutorial on support vector regression," *Stat. and Comput.*, vol. 14, no. 3, pp. 199–222, 2004.
- [65] S. Le Cessie and J. C. Van Houwelingen, "Ridge estimators in logistic regression," *Appl. Stat.*, pp. 191–201, 1992.
- [66] R. Tibshirani, "Regression shrinkage and selection via the lasso," *J. Roy. Stat. Soc. B Met.*, pp. 267–288, 1996.
- [67] G. Rätsch, T. Onoda, and K.-R. Müller, "Soft margins for adaboost," *Mach. Learn.*, vol. 42, no. 3, pp. 287–320, 2001.
- [68] L. Bottou, "Large-scale machine learning with stochastic gradient descent," in *Proceedings of COMPSTAT'2010*. Springer, 2010, pp. 177–186.
- [69] H. Zou and T. Hastie, "Regularization and variable selection via the elastic net," *J. R. Stat. Soc. B*, vol. 67, no. 2, pp. 301–320, 2005.
- [70] B. Efron, T. Hastie, I. Johnstone, R. Tibshirani *et al.*, "Least angle regression," *Ann. Stat.*, vol. 32, no. 2, pp. 407–499, 2004.



agnostics, prognostics.

Chong Zhang (S'16) received the B.Eng. degree in engineering from Harbin Institute of Technology, China, and the M.Sc. degree from National University of Singapore in 2011 and 2012, respectively. She is currently a Ph.D. student in Electrical and Computer Engineering at National University of Singapore as well as a Research Engineer in National University of Singapore.

Her research interests include computational intelligence, machine/deep learning, data science, multi-objective optimization and their applications in di-



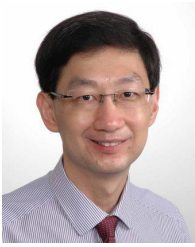
tem, Neural network Applications and Industrial Automation, Modeling and control of Mechanical Systems, Tool Condition Monitoring, AI techniques in monitoring and Diagnostics.

Geok Soon Hong received the B.Eng. degree in Control Engineering in 1982 from University of Sheffield, UK. He was awarded a university scholarship to further his studies and obtained a Ph.D. degree in control engineering in 1987. The topic of his research was in stability and performance analysis for systems with multi-rate sampling problems. He is now an Associate Professor at the Department of Mechanical Engineering, National University of Singapore (NUS), Singapore. His research interests are in Control Theory, Multirate sampled data system, Neural network Applications and Industrial Automation, Modeling and control of Mechanical Systems, Tool Condition Monitoring, AI techniques in monitoring and Diagnostics.



Dr. Zhou was a recipient of the 2011 Best Application Paper Award in the 8th Asian Control Conference, and the 2012 Best Paper Award in the International Association of Science and Technology for Development International Conference on Engineering and Applied Science.

Jun-Hong Zhou received the Ph.D. degree from Nanyang Technological University, Singapore, with a focus on advanced feature extraction and selection in condition-based maintenance. She is currently a Principle Researcher with the Singapore Institute of Manufacturing Technology (SIMTech), Agency for Science, Technology and Research, Singapore, and also the initiative lead in maximizing overall equipment effectiveness. She has been involved in a number of research and industry projects in process monitoring and control, sensing and advanced signal processing, and data analytics and data mining, since 1996. She has been actively involved with industries, including the SCADA system, sensing and measurement for machine tooling condition, intelligent modeling for equipment health prognostics, and process monitoring and product control in manufacturing processes and intelligent systems to maintain serviceability of manufacturing equipment. She has authored over 60 technical papers.



Kay Chen Tan (SM'08–F'14) received the B.Eng. degree (First Class Hons.) in electronics and electrical engineering and the Ph.D. degree from the University of Glasgow, Glasgow, U.K., in 1994 and 1997, respectively.

He is a Professor with the Department of Computer Science, City University of Hong Kong, Hong Kong. He has published over 100 journal papers and over 100 papers in conference proceedings, and co-authored five books. His current research interests include computational and artificial intelligence,

with applications to multiobjective optimization, scheduling, automation, data mining, and games.

Dr. Tan was a recipient of the 2012 IEEE Computational Intelligence Society Outstanding Early Career Award for his contributions to evolutionary computation in multiobjective optimization. He was the Editor-in-Chief of the IEEE COMPUTATIONAL INTELLIGENCE MAGAZINE from 2010 to 2013. He is currently the Editor-in-Chief of the IEEE TRANSACTIONS ON EVOLUTIONARY COMPUTATION. He serves as an Associate Editor/Editorial Board Member of over 15 international journals, such as the IEEE TRANSACTIONS ON CYBERNETICS, the IEEE TRANSACTIONS ON COMPUTATIONAL INTELLIGENCE AND AI IN GAMES, *Evolutionary Computation*, *the European Journal of Operational Research*, *the Journal of Scheduling*, and *the International Journal of Systems Science*.



Hian-Leng Chan received his B. Eng in Mechanical Engineering from NUS, and his M. S. and PhD from Department of Aeronautics & Astronautics Stanford University in 1998 and 2005 respectively. He is currently Team Lead for Shop-floor Health Management and Group Head for Manufacturing Execution & Control Group at Singapore Institute of Manufacturing Technology, A*STAR. His previous experience includes aerodynamics research at DSO and structural health monitoring development at Accellent Technologies, Inc. He had previously

worked in several areas of condition monitoring using vibration, sound, electrical current and acousto-ultrasonics. His research interests are machine learning, data analytics for feature extraction, fault diagnosis, condition monitoring, fault classification and for predictive maintenance.



Haizhou Li (M'91–SM'01–F'14) received the B.Sc., M.Sc., and Ph.D degree in electrical and electronic engineering from South China University of Technology, Guangzhou, China in 1984, 1987, and 1990 respectively. Dr Li is currently a Professor at the Department of Electrical and Computer Engineering, National University of Singapore (NUS). He is also a Conjoint Professor at the University of New South Wales, Australia. His research interests include automatic speech recognition, speaker and language recognition, and natural language process-

ing.

Prior to joining NUS, he taught in the University of Hong Kong (1988-1990) and South China University of Technology (1990-1994). He was a Visiting Professor at CRIN in France (1994-1995), Research Manager at the Apple-ISS Research Centre (1996-1998), Research Director in Lernout & Hauspie Asia Pacific (1999-2001), Vice President in InfoTalk Corp. Ltd. (2001-2003), and the Principal Scientist and Department Head of Human Language Technology in the Institute for Infocomm Research, Singapore (2003-2016).

Dr Li is currently the Editor-in-Chief of IEEE/ACM TRANSACTIONS ON AUDIO, SPEECH AND LANGUAGE PROCESSING (2015-2018), a Member of the Editorial Board of *Computer Speech and Language* (2012-2018). He was an elected Member of IEEE Speech and Language Processing Technical Committee (2013-2015), the President of the International Speech Communication Association (2015-2017), the President of Asia Pacific Signal and Information Processing Association (2015-2016), and the President of Asian Federation of Natural Language Processing (2017-2018). He was the General Chair of ACL 2012 and INTERSPEECH 2014.

Dr Li is a Fellow of the IEEE. He was a recipient of the National Infocomm Award 2002 and the Presidents Technology Award 2013 in Singapore. He was named one of the two Nokia Visiting Professors in 2009 by the Nokia F

Huan Xu is a PhD candidate in Mechanical Engineering in National University of Singapore. She received the B. E. degree from Xian JiaoTong University, China, in 2016.

Her main areas of research is the application of neural networks and machine learning in tool condition monitoring. She focuses on tool condition diagnostics and estimation by using AI techniques.

